An analytic scaling relation for the maximum tokamak elongation against n=0 MHD resistive wall modes

Jungpyo Lee[1], Jeffrey Freidberg[1], Antoine Cerfon[2] and Martin Greenwald[1]

[1]MIT Plasma Science and Fusion Center, USA
[2]NYU Courant Institute of Mathematical Science, USA

Corresponding Author: jungpyo@psfc.mit.edu

Abstract:

In this study, the maximum achievable elongation in a tokamak as determined theoretically by the n=0 MHD resistive wall mode is investigated theoretically. A highly elongated plasma is desirable in order to increase plasma pressure and energy confinement to maximize fusion power output. However, there is a limit to the maximum achievable elongation which is set by vertical instabilities driven by the n=0 MHD mode. This limit can be increased by optimizing several parameters characterizing the plasma and the wall. The purpose of our study is to explore how and to what extent this can be done. Specifically, we extend many earlier calculations of the n=0 mode to determine the maximum elongation as a function of dimensionless parameters describing (1) the plasma profile (β_p and l_i), (2) the plasma shape (ϵ and δ), (3) the wall radius (b/a) and (4) most importantly the feedback system capability parameter $\gamma\tau$. We make use of a new formulation of n=0 MHD theory developed in our recent study [Freidberg et. al. 2015; Lee et. al. 2015] that reduces the 2-D stability problem into a 1-D problem. This method includes all the physics of the ideal MHD axisymmetric instability but it reduces the computation time significantly so that many parameters can be explored during the optimization process. We have explored a wide range of parameter space to find the optimized shape against n=0 mode. Perhaps the most useful final result is a simple analytic fit to the simulations which gives the maximum elongation and corresponding optimized triangularity as functions $\kappa(\epsilon, \beta_p, l_i, b/a, \gamma\tau)$ and $\delta(\epsilon, \beta_p, l_i, b/a, \gamma\tau)$. These theoretically obtained scaling relations can be useful for determining optimum plasma shape in current experiments and future tokamak designs.

1 Introduction

A highly elongated tokamak is desirable in order to increase plasma pressure and energy confinement, as verified in many experiments [1] and numerical simulations [2]. In the design of ITER, the confinement time τ_E was estimated by experimentally derived empirical scaling relations. These relations, plus the well-known Troyon MHD beta limit, show a strong dependency on the elongation parameter κ (i.e. $\tau_E \propto \kappa^{0.7}$ [3] and $\beta \propto (1 + \kappa^2)$ [4]). The maximum value of elongation is likely limited by axisymmetric (n=0) MHD

resistive wall modes, which drive the vertical instability. However, the maximally achievable elongation is not well formulated theoretically, particularly when the properties of the feedback system are included. In this study, we derive analytical scaling relations for the maximum elongation against n=0 mode in terms of the critical physics and engineering parameters. The analysis is based on the theory and numerical method developed recently [5, 6].

There have been many numerical investigations of the n=0 MHD stability using different models (e.g. plasma surrounded by a perfectly conducting wall [7] or by a resistive wall [8]). However, these studies do not directly include the impact of the feedback system. In our analysis, the realistic engineering system controlling the vertical instability in experiments is modeled by the introduction of a feedback parameter $\gamma\tau$ [5]. A new numerical formulation has been developed [6] to efficiently compute the instability making use of the new theory including the resistive wall plus the parameter $\gamma\tau$ [5]. Because our numerical formation reduces the 2-D stability problem to an equivalent 1-D problem, it is computationally inexpensive thus allowing us to explore several dimensions in multi-parameter space and obtain the analytic scaling relations by running thousands of simulations.

A key additional feature of the present simulations as compared to the previous studies in [6] is the generalization of the plasma equilibrium density and pressure profiles as inputs to the simulations. In [5, 6], the plasma profiles are restricted to the simple "Solov'ev profile" which is a purely analytical model [9]. However, the Solov'ev pressure and current profiles are somewhat flat radially compared to typical experimentally profiles. Specifically, the Solov'ev profile has an internal inductance of about $l_i \simeq 0.4$, which is considerably smaller than the typical experimentally measured profiles characterized by $l_i > 0.7$. For arbitrary plasma profiles we use the iterative solver for second-order elliptic partial differential equation, ECOM [10], to calculate the equilibrium poloidal magnetic flux Ψ satisfying the Grad-Shafranov equation,

$$\Delta^\star \Psi = -\left(\mu_0 R^2 \frac{\partial p}{\partial \Psi} + \frac{1}{2}\frac{\partial F^2}{\partial \Psi}\right) \tag{1}$$

and the perturbed poloidal magnetic flux ψ satisfying the following equation,

$$\Delta^\star \psi = -\left(\mu_0 R^2 \frac{\partial^2 p}{\partial \Psi^2} + \frac{1}{2}\frac{\partial^2 F^2}{\partial \Psi^2}\right)\psi. \tag{2}$$

By computing numerical solutions for ψ and its normal derivative $\mathbf{n}\cdot\nabla\psi$ at the plasma boundary for each poloidal Fourier mode, we can use the general formulation in [6] for $\delta W = 0$ for arbitrary plasma profiles. If m is the number of poloidal Fourier modes used to decompose the perturbed flux ψ, the computational cost is about m times larger than that of Solov'ev equilibrium in [5]. Nevertheless, the stability formulation still only requires the solution to two 1-D problems at the two radial interfaces (plasma-vacuum and vacuum-wall). Thus, it is much more efficient than solving the full 2-D stability problems directly.

As described in [6], we find a set of parameters which satisfy $\delta W = 0$ including the feedback control parameter $\gamma\tau$. Using this set of parameters, the maximum elongation κ can be determined numerically in terms of the following six critical dimensionless physics parameters: (1) beta poloidal ($\beta_p = 2\mu_0 \int_V p d\mathbf{r}/B_p^2$), (2) internal inductance ($l_i = 2\int_V B_p^2 d\mathbf{r}/(\mu_0^2 I_\phi^2 R_0)$), (3) inverse aspect ratio (ϵ), (4) triangularity (δ), (5) the ratio of wall radius to the plasma radius (b/a) and (6) the feedback system performance parameter $\gamma\tau$. Here, the parameters for the shape (κ, δ, and ϵ) follow the definitions in [11]. For simplicity, we change the size of the wall distance by varying only one parameter Δ_o defined by $b/a = (1 + \Delta_o)$. We fix the shape of the wall relative to the plasma interface shape by keeping the ratio of gaps in each direction $\Delta_o = \Delta_i = (1/3)\Delta_v$ constant: these ratios are similar to those of many existing tokamak wall shapes [6]. Here Δ_o, Δ_i and Δ_v are the outer, inner, and vertical gap between the plasmas and wall, respectively.

In Section 2, we describe how to select an accurate but simple fitting model for $\kappa(\beta_p, l_i, \epsilon, \delta,\ b/a, \gamma\tau)$. In Section 3, the analytic scaling results are presented and some remarkable features of the scaling laws are discussed in Section 4.

2 Scaling model

To reduce the parameter space in the scaling relation, we prefix the triangularity by $\delta = \delta_m$ in the model. As has been shown in [6], the maximum stable elongation usually occurs at an optimized value of triangularity. However, some comments are in order. (1) While there is an optimum δ, the corresponding κ_{max} is somewhat flat. Thus κ_{max} is only slightly sensitive to the value of δ. (2) In general, the optimum δ increases with ϵ, β_p, and l_i. Eventually, a sufficiently large value of any of these parameters leads to an optimum $\delta \simeq 0.8$. When this occurs, the well-known Miller cross section [11] used in the simulations breaks down in the sense that the plasma shape no longer remains convex - it assumes instead a bean shape. To avoid this difficulty, when the critical δ exceeds 0.7, we simply fix δ_m at this value. This also helps because our equilibrium solver starts to loose accuracy at large value of δ [10]. To summarize, when the optimum δ is less than 0.7, we use $\delta_m = \delta_{opt}$ to calculate κ_{max} . When δ_{opt} approaches and attempts to exceed the value 0.7, we set $\delta_m = 0.7$. In view of the flatness of the δ_{opt} curve this should not lead to a significant error.

In this section, for the clarity of the presentation, we discuss the scaling models without specifying the numerical values for the various factors and exponents. In section 3, we will then specify all the coefficients and exponents we obtained from many simulations.

2.1 The optimum triangularity

Based on the discussion above, we model the dependency of κ on δ by a quadratic form for simplicity,

$$\kappa = \begin{cases} \kappa_{max} - \kappa_\delta(\delta - \delta_m)^2 & \text{for } \delta_m = \delta_{opt} \le 0.7 \\ \kappa_{max} & \text{for } \delta_m = 0.7 < \delta_{opt}. \end{cases} \tag{3}$$

Here the optimal triangularity δ_{opt}, the coefficient κ_{opt} as well as κ_{max} have substantial dependence on ϵ, l_i, β_p, Δ_o, and $\gamma\tau$. The existence of the optimal triangularity is largely due to the competing effects between the pressure driven term and the line bending term in δW, which are sensitive to the plasma profiles. From our simulation results we have found that a good fit to the numerical data for the triangularity coefficients is given by

$$\begin{aligned} \delta_{opt} &= \hat{\delta} l_i^{\alpha_1} \beta_p^{\alpha_2} \epsilon^{\alpha_3}, \\ \kappa_\delta &= \hat{\kappa} l_i^{\beta_1} \beta_p^{\beta_2} \epsilon^{\beta_3}, \end{aligned} \tag{4}$$

where $\alpha_3(l_i, \beta_p, \gamma\tau, \Delta_o) = \alpha_4 + \alpha_5 l_i + \alpha_6 \beta_p + \alpha_7(\gamma\tau) + \alpha_8(1+\Delta_o)$ and $\beta_3(l_i, \beta_p, \gamma\tau, \Delta_o) = \beta_4 + \beta_5 l_i + \beta_6 \beta_p + \beta_7(\gamma\tau) + \beta_8(1+\Delta_o)$. Note the complex behavior of the ϵ coefficient. Also keep in mind that these relations are valid for $\delta_{opt} \leq 0.7$.

2.2 The large aspect ratio dependence of the maximum elongation

Let us now assume that the triangularity has been set to its optimum value as defined in Eq. (3). We turn our attention to the important question of the maximum achievable elongation, that is, the value of κ_{max}. Our numerical results show that the maximum elongation at the optimal triangularity κ_{max} can be accurately modeled by

$$\kappa_{max} = \kappa_0 + \kappa_1 \left(\frac{2\epsilon}{1+\epsilon^2} \right)^2. \tag{5}$$

Consider first the coefficient κ_0 which represents the maximum elongation in the limit of large aspect ratio. In this limit, when the wall is at infinity, the optimal shape approaches a circle corresponding to $\delta_{opt} \to 0$ and $\kappa_0 = 1$. Mathematically, the wall can be moved to infinity several ways: $\Delta_o \to \infty$, $l_i \to \infty$, and $\gamma\tau \to 0$. For finite values of these parameters a good fit to the numerical simulations is obtained by assuming that κ_0 scales as

$$\kappa_0 = 1.0 + \hat{\kappa}_0 \frac{(\gamma\tau)^{\nu_1}}{l_i^{\nu_2}(1+\Delta_o)^{\nu_3}}. \tag{6}$$

Note that the dependence of κ_0 on β_p is very weak and can be ignored with a minimal loss in accuracy.

2.3 The finite aspect ratio dependence of the maximum elongation

The aspect ratio dependence of the maximum elongation is determined by the coefficient κ_1 and the functional dependence on ϵ assumed in Eq. (5). Observe that as $\epsilon \to 0$, the maximum elongation is proportional to ϵ^2, as may be expected in a previous result on the natural elongation of tokamaks [12]. Also, as $\epsilon \to 1$, the maximum elongation saturates. The numerical simulations show that an accurate model for κ_1 can be written as

$$\kappa_1 = \hat{\kappa}_1 l_i^{\mu_1} \beta_p^{\mu_2} (\gamma\tau)^{\mu_3} (1+\Delta_o)^{\mu_4}. \tag{7}$$

3 Fitting results

3.1 Condition for optimal triangularity

We have found that optimal triangularity generally increases as ϵ, l_i or β_p increases. Taking the log of the factors in Eq. (4) and using a least square fitting, we obtain the fitting parameters by

$$\delta_{opt} = 2.30 l_i^{1.27} \beta_p^{-0.01} \epsilon^{(1.21-0.76 l_i - 1.22\beta_p - 0.001(\gamma\tau) + 1.21(1+\Delta_o))}, \tag{8}$$

$$\kappa_\delta \;=\; 0.27 l_i^{-2.88} \beta_p^{0.10} \epsilon^{(0.45+0.24 l_i - 0.23\beta_p + 0.19(\gamma\tau) - 0.75(1+\Delta_o))}. \tag{9}$$

Because the quadratic model in Eq. (3) is actually too simple to find a very accurate fit, the errors of the fitting are non-negligible: the standard deviation for the fits are $\sigma = 0.09$ in Eq. (8) and $\sigma = 0.31$ in Eq. (9). Even so, because of the flatness of the κ vs. δ curve, the errors do no produce much of a change in κ_{max}.

Still, κ_δ in Eq. (9) is a good indicator of the sensitivity of κ on δ. The formula shows a robust tendency for κ_δ to decrease as l_i increases. Physically this can be explained by follows: as l_i increases, the plasma current density is more concentrated in the core, and the effect of surface triangularity on the $n = 0$ MHD mode is reduced.

Figure 1-(a) shows the contour plot of optimal triangularity obtained in many simulations in terms of β_p and l_i, and Figure 1-(b) shows the contour of the fitting formula of δ_{opt} which will be explained in Eq. (8). As discussed in Section 2, if the optimal triangularity δ_{opt} is comparable to or large than the value 0.7, there is no optimal triangularity. Roughly speaking, the optimal triangularity tends to exceed 0.7 if $l_i \geq 1.0$ or $\beta_p \geq 1.4$ for $\epsilon = 0.3$, $\gamma\tau = 1.5$ and $\Delta_o = 0.1$.

3.2 Fitting of κ_0

As shown in Figure 2-(a), the parameters of the scaling relation for κ_0 in Eq. (6) is calculated by fitting the simulation results of κ at $\epsilon = 0.01$ and $\delta = 0.0$. The result is

$$\kappa_0 \;=\; 1.0 + 0.54 l_i^{-0.68} (\gamma\tau)^{0.62} (1+\Delta_o)^{-3.52}, \tag{10}$$

where the standard deviation of the fitting is quite low ($\sigma = 0.003$).

3.3 Fitting of κ_1

The coefficient for the ϵ dependence, κ_1 in Eq. (7), can be estimated by the difference between $\kappa_{max}(\epsilon = 0.01)$ and $\kappa_{max}(\epsilon = 0.6)$, where $\epsilon = 0.6$ is the maximum value of our interest in this analysis. As shown in Figure 2-(a), κ_1 is obtained by

$$\kappa_1 \;=\; 0.60 l_i^{0.24} \beta_p^{0.02} (\gamma\tau)^{0.12} (1+\Delta_o)^{-0.44}, \tag{11}$$

where the standard deviation of the fitting is reasonably low ($\sigma = 0.05$). Here, the constant 0.35 in Eq. (11) is given by $0.27/(2\epsilon/(1+\epsilon^2))^2$ for $\epsilon = 0.6$.

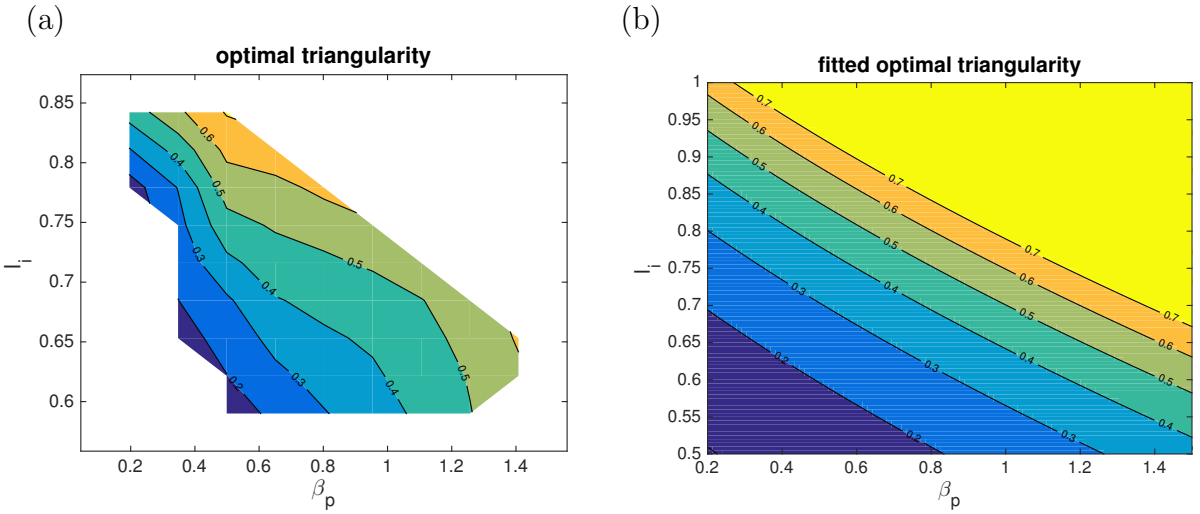

FIG. 1: Contour of optimal triangularity δ_{opt} in terms of l_i and β_p using a) simulation result and (b) fitted formula in Eq. (8) for $\gamma\tau = 1.5$, $\Delta_o = 0.1$ and $\epsilon = 0.3$. The upper-right white space in (a) indicates the parameters having no optimal triangularity in the simulations.

Using the combined fitting parameter for κ_0 and κ_1 in Eq. (10) and (11), the simple scaling in Eq. (5) results in a good fit for all simulation results in parameter space of ϵ, l_i, β_p, Δ_o, and $\gamma\tau$. Figure 3 shows the fitting of κ_{max} in Eq. (5) characterized by the deviation $\sigma = 0.11$.

4 Discussion

We conclude by noting several points for the scaling laws obtained in Section 3:
(1) As β_p increases or l_i increases, δ_{opt} increases. Eq. (8) shows that β_p affects only the ϵ dependent factor in δ_{opt}, while l_i affects both the ϵ dependent factor and the factor independent of ϵ. The ϵ dependent factor is mainly due to the Shafranov shift, which is approximately proportional to the theoretical value in the low ϵ limit (i.e. $-1.22\beta_p - 0.76l_i \sim -1.22(\beta_p + 0.5l_i)$ in Eq. (8)).
(2) The sensitivity of κ on δ is reduced by increasing l_i, as shown by the decrease of κ_δ in Eq. (9).
(3) Eq. (10) and Eq. (11) show that l_i affects both κ_0 and κ_1, β_p primarily affects κ_1, and $\gamma\tau$ and Δ_o primarily affects κ_0,

References

[1] Lomas P. J. and JET Team,"The variation of confinement with elongation and triangularity in ELMy H-modes on JET", Plasma Physics and Controlled Fusion

(a) (b)

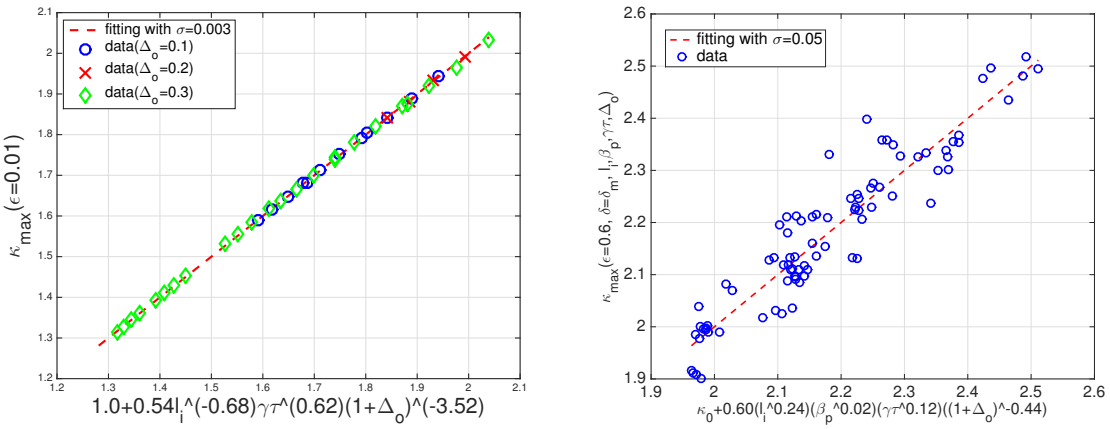

FIG. 2: Fitting of (a) κ_0 by $\kappa_{max}(\epsilon = 0.01)$ and (b) κ_1 by $\kappa_{max}(\epsilon = 0.6)$

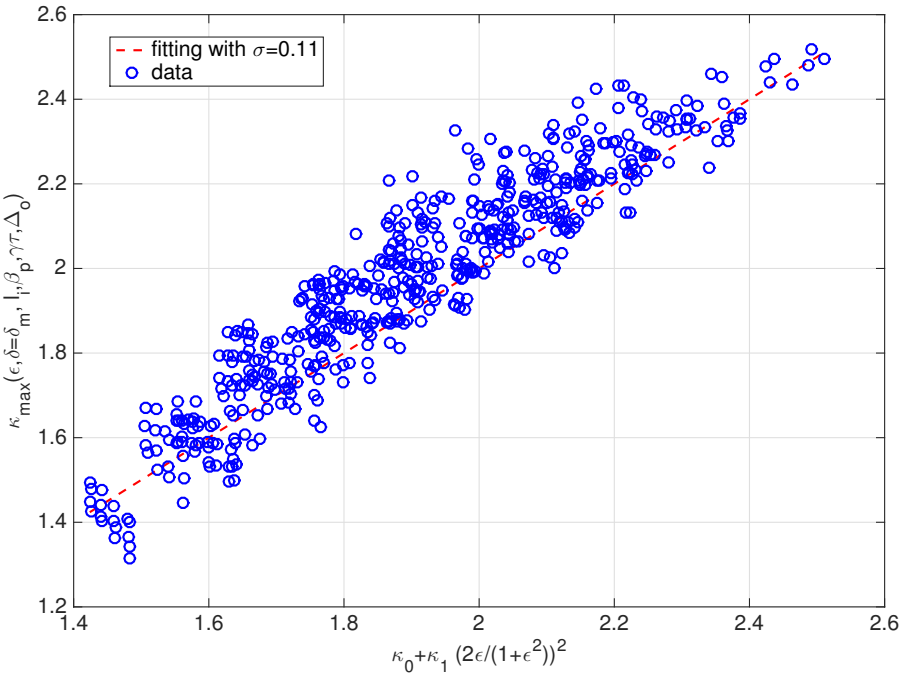

FIG. 3: Fitting of κ_{max} using Eq. (5) with κ_0 and κ_1 in Eq. (10) and (11)

42 (2000) B115.

[2] Kinsey, J. E., et. al., "The effect of plasma shaping on turbulent transport and E B shear quenching in nonlinear gyrokinetic simulations", Phys. Plasmas **14** (2007) 102306.

[3] ITER Physics Expert Groups on Confinement and Transport and Confinement Modelling and Database, ITER Physics Basis Editors and ITER EDA, Nucl. Fusion **39** (1999) 2175.

[4] Troyon, F., et. al., "MHD-Limits to Plasma Confinement", Plasma Phys. Control. Fusion **26** (1984) 209.

[5] Freidberg, J. P., et. al.,"Tokamak elongation: how much is too much? Part 1. Theory", Journal of Plasma Physics **81** (2015) 515810607.

[6] Lee, J. P., et. al.,"Tokamak elongation: how much is too much? Part 2. Numerical results", Journal of Plasma Physics **81** (2015) 515810608.

[7] Laval, G. and Pellat, R., Controlled Fusion and Plasma Physics (Proc. 6th Europ. Conf. Moscow 1973) **2** (1973) 640.

[8] Wesson, J. A., Controlled Fusion and Plasma Physics (Proc. 7th Europ. Conf. Lausanne 1975) **2** (1975) 102.

[9] Solovev, L. S., "The theory of hydromagnetic stability of toroidal plasma configurations", Sov. Phys.- JETP **26** (1968) 400.

[10] Lee, J. P. and Cerfon, A. "ECOM: A fast and accurate solver for toroidal axisymmetric MHD equilibria", Computer Physics Communications **190** (2015) 72.

[11] Miller, R. L., et. al., "Noncircular, finite aspect ratio, local equilibrium model", Physics of Plasmas **5** (1998) 973.

[12] Hakkarainen, S. P., et. al.,"Natural elongation and triangularity of tokamak equilibria", Phys. Fluids B **2** (1990) 1565.